
Diagnosis and surgical treatment of associated papillary lung adenocarcinoma to canine distemper - case report

Diagnóstico e tratamento cirúrgico de adenocarcinoma pulmonar papilar associado à cinomose canina – relato de caso

José Roberto da Silva Júnior

ORCID: <https://orcid.org/0009-0003-7523-5293>
Triângulo University Center (UNITRI), Brasil
E-mail: juniorjrj.80@gmail.com

Júlio César Basso Machado

ORCID: <http://orcid.org/0000-0003-4747-3975>
Federal University of Uberlândia (UFU), Brazil
E-mail: julio.basso@yahoo.com.br

Laiz Basso Machado

ORCID: <https://orcid.org/0000-0003-4342-421x>
Federal University of Uberlândia (UFU), Brazil
E-mail: laiz_basso@hotmail.com

Taynara Tuanne Lima Pereira

ORCID: <https://orcid.org/0009-0001-1149-4291>
Federal University of Uberlândia (UFU), Brazil
E-mail: ttuanelima@gmail.com

Nicolle Pereira Soares

ORCID: <http://orcid.org/0000-0002-4135-1435>
Federal University of Uberlândia (UFU), Brazil
E-mail: nicolle.pereira@hotmail.com

Elisa Ferreira Theodoro Boleli

ORCID: <https://orcid.org/0009-0009-5433-7948>
Veterinary Imaging Center, Brasil
E-mail: elisafb.vet@gmail.com

Isaura Maria Ferreira

ORCID: <http://orcid.org/0000-0002-7075-8971>
Federal Institute of Triângulo Mineiro (IFTM), Brasil
E-mail: isaura@iftm.edu.br

Leandro Willian Borges

ORCID: <https://orcid.org/0000-0002-4598-2568>
Federal University of Uberlândia (UFU), Brazil
E-mail: leandro_william@hotmail.com

Douglas Alves Pereira

ORCID: <https://orcid.org/0000-0001-8426-7535>
Federal University of Uberlândia (UFU), Brazil
E-mail: douglas.vet1@gmail.com

RESUMO

As neoplasias pulmonares em cães possuem etiologia multifatorial, sendo os animais com 10 anos ou mais os mais acometidos, sem predisposição sexual ou racial. O adenocarcinoma é o tipo de câncer mais comum e representa cerca de 80% dos casos. O objetivo deste estudo foi descrever um caso de um cão de 11 anos de idade, sem raça definida (SRD), com adenocarcinoma papilífero de pulmão e vírus da cinomose canina. O exame clínico revelou escore de condição corporal (ECC: 5,0), normocárdico, taquipneico, normotérmico, desidratação leve (5 - 6%), hiporexia, mucosas hipocoloridas, normodipsia, normúria e normoquesia. Foram realizados exames hematológicos (hemograma, bioquímica), evidenciando inicialmente leucocitose e anemia regenerativa. Exames de imagem de tórax (radiografia) e tomografia computadorizada (TC) evidenciaram nódulo, com aproximadamente 7cm de circunferência, na porção ventral do lobo pulmonar caudal direito. O tratamento foi por toracotomia para excisão do nódulo. O material excisado foi enviado para diagnóstico histopatológico e imunohistoquímico, que confirmou o diagnóstico de adenocarcinoma pulmonar. A infecção pelo vírus da cinomose foi confirmada pela identificação do corpúsculo de Lentz, encontrado na amostra de sangue durante a contagem diferencial de leucócitos, quando o animal foi devolvido para reavaliação. O animal não respondeu ao tratamento e faleceu 48 horas após o diagnóstico de cinomose, em resposta à parada cardiorrespiratória, 12 dias após a retirada do nódulo. A infecção pelo vírus da cinomose levou a um prognóstico desfavorável e impossibilitou o tratamento pós-cirúrgico, culminando com a morte do animal.

Palavras-chave: Coinfecção viral; Neoplasia Pulmonar; Oncologia; Sobrevivência.

ABSTRACT

Lung neoplasms in dogs have a multifactorial etiology, and animals aged 10 or older are the most affected, with no sexual or racial predisposition. Adenocarcinoma is the most common type of cancer and represent around 80% of the cases. The aim of this study was to describe a case of an 11-year-old dog of no defined breed (SRD) with papillary lung adenocarcinoma and canine distemper virus. Clinical examination revealed a body condition score (BCS: 5.0), normocardial, tachypneic, normothermic, mild dehydration (5 - 6%), hyporexia, hypocolored mucous membranes, normodipsia, normuria and normoquesia. Hematological tests (blood count, biochemistry) were carried out, initially showing leukocytosis and regenerative anemia. Imaging tests of the chest (x-ray) and computed tomography (CT) showed a nodule, with approximately 7cm in circumference in the ventral portion of the right caudal lung lobe. Treatment was by thoracotomy to excise the nodule. The excised material was sent for histopathological and immunohistochemical diagnosis, which confirmed the diagnosis of lung adenocarcinoma. Infection with the distemper virus was confirmed by the identification of the Lentz corpuscle, which was found in the blood sample during the differential leukocyte count, when the animal was returned for re-evaluation. The animal did not respond to treatment and died 48 hours after the diagnosis of distemper, in response to cardiorespiratory arrest, 12 days after the removal of the nodule. Infection with the distemper virus led to an unfavorable prognosis and made post-surgical treatment impossible, culminating in the animal's death.

Keywords: Viral co-infection; Pulmonary Neoplasia; Oncology; Survival.

INTRODUCTION

Various conditions can affect the organs of the respiratory system in pets, including pulmonary conditions, affecting around 4% of the cases of this system and can be originated by infection, circulatory disorders or pleural conditions, as well as primary or metastatic neoplastic conditions (ROCHA et al., 2013).

In animals, regarding lung neoplasms, tumors in dogs can be divided into different histological types based on the microscopic characteristics of the tumor tissue. Some of the most common types of lung tumors in dogs include: pulmonary adenocarcinoma, a type of tumor that originates from the glandular cells of the lung tissue; squamous cell carcinoma, a tumor that originates from the squamous cells of the respiratory mucosa; large cell carcinoma, a tumor that presents large, pleomorphic cells; small cell carcinoma, a tumor with small, round cells, similar to small cell carcinoma in humans; and neuroendocrine tumor, which includes tumors such as small cell neuroendocrine carcinoma and large cell carcinoma with neuroendocrine characteristics. (WILSON; DEVARAJ, 2017; MEUTEN, 2020).

The origin of lung neoplasms is multifactorial, and the animals that develop this pathology have an average age of 10 and 11 years, without racial or sexual predisposition (DA SILVA et al., 2012; PEREIRA et al., 2019). In addition, another cause of the origin of lung neoplasms can be explained by the close contact of dogs with humans and exposure to similar environmental risk factors, such as air pollutants from urban life (LEANDRO et al., 2015) and passive smoking (LORCH et al., 2019; DEVARAKONDA et al., 2021) and gene mutation (LORCH et al., 2019). Lung adenocarcinoma is the most diagnosed malignant neoplasm accounting for around 70 to 80% of case and is divided into two patterns: papillary and bronchoalveolar which thrive in epithelial glandular tissues (SALVADO, 2010; PEDROSO et al., 2010; MANIAM et. al, 2018).

Canine lung tumors can be identified during the investigation of respiratory or other non-specific symptoms (LEE et al., 2020). Animals affected by lung adenocarcinoma commonly present dyspnea, a chronic cough, lethargy, weight loss, anorexia, occasional vomiting and, in the most aggressive and terminal cases, paraneoplastic syndromes (MANIAM et. al, 2018).

Imaging tests show the location of the tumors, with X-rays in three projections allowing nodules to be seen in variable image patterns and solitary nodular densities in

lung lobes. Computed tomography (CT) allows a more reliable assessment of the size, possible areas of calcification, number and density of the lesion (PEREIRA et al., 2019; ABLE et al., 2021), while magnetic resonance imaging allows sharper, high-definition images to be captured, regardless of the affected tissue, without using radiation (KISHI et al., 2014; PALLADINO et al., 2016).

Histopathological examination provides a confirmatory diagnosis, through microscopic analysis of the affected tissue to detect lesions characteristic of adenocarcinoma (VIGNOLI et al., 2020), as well as molecular analysis methods, such as immunohistochemistry, which allows confirmation of the diagnosis by detecting specific antigens, favoring a prognostic and oncological assessment of the patient affected by the neoplasm (IGUCHI et al., 2019; KITA et al., 2022).

The standard treatment used is surgical, performing total or partial excision of the affected lobe by intercostal thoracotomy or sternotomy, and more recently video surgery techniques have been developed (KANAI et al., 2019). Associated with surgical treatment, chemotherapy is recommended and the most used pharmacological bases include cisplatin, carboplatin, etoposide, cyclophosphamide, doxorubicin, vincristine sulfate, lomustine, ifosfamide, paclitaxel, docetax and others (DALECK; DE NARDI, 2016). In addition to the chemotherapy drugs mentioned above, another option is electrochemotherapy combined with electrical pulses, which acts by forming pores in the cell membrane of the tumor cell, facilitating the penetration of the chemotherapy drug and thus increasing the absorption of the drug through the cell membranes, seeking greater efficacy in the treatment of affected animals (VALENTI et al., 2021).

The goal of this study to describe a case of Papillary Lung Adenocarcinoma and carrier of the distemper virus in an 11-year-old male dog of no defined breed (SRD), treated at a private clinic in the city of Uberlandia, Minas Gerais, highlighting its clinical characteristics, diagnosis, treatment used, prognosis and survival time.

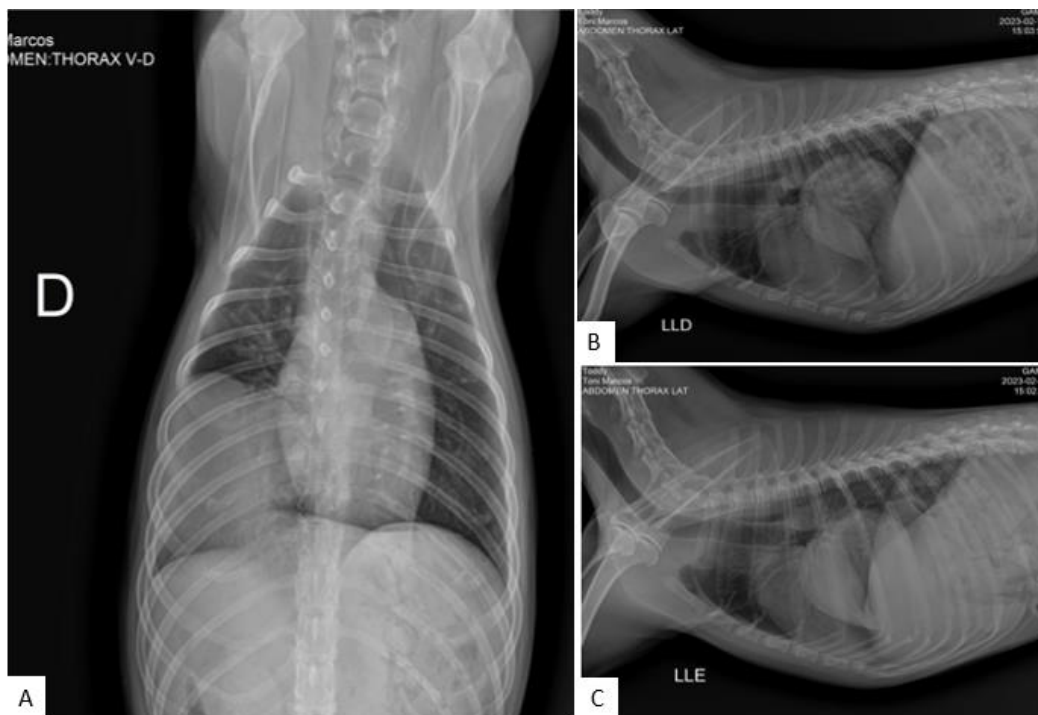
CASE REPORT

A male, 11-year-old, SRD, uncastrated, 6.100 kg dog with a history of vomiting episodes, not eating well, weight loss, increased respiratory effort and a dry cough for approximately 10 day visited the veterinary clinic in the city of Uberlandia, state of Minas Gerais, Brazil, on 2023/02/13. The animal lived in a house with no access to the street and

cohabited with another healthy dog. The vaccination protocol was overdue in terms of polyvalent immunization, rabies was up to date, deworming was up to date, there was no control of ectoparasites and his diet was predominantly based on "Premium" dry food. On general clinical examination, the animal had a body condition score (ECC - 5.0), was normocardic (120bpm) with hypophonesis, tachypneic (48mrpm), normothermic (38.7°C), mildly dehydrated (5 - 6%), with a capricious appetite, hypochromic mucous membranes, normodipsia, normuria and normoquesia. Hematological tests such as a blood count and biochemistry were carried out, as well as chest X-rays. The erythrogram showed no alterations, the leukogram showed high leukocytosis (34,300mm³) followed by neutrophilia (segmented 31,899mm³ and rods 686mm³), the platelet count (433,000 mm³) was normal. Biochemistry (creatinine, ALT, FA) was normal.

Orthogonal chest X-rays were taken in three projections: right laterolateral, left laterolateral and ventrodorsal, showing an area with partially defined limits and greater radiopacity, approximately 7cm in diameter, located between the 6th and 11th right intercostal spaces, in the right caudal pulmonary lobe. The cardiac silhouette was within normal radiographic standards, the lumen and tracheal pathway were preserved, there was a slight amount of gaseous content in the esophageal pathway (aerophagia), degeneration of the costal cartilages and osteoarthritis of the costochondral joints (suggestive of senescence), deforming ventral spondylosis at T6-7 (suggestive of a degenerative process) and heterogeneous content (suggestive of food content) in the gastric cavity The bony structures of the rib cage were preserved (figure 1).

Figure 1. First chest X-ray in three projections of a SRD dog. (A) ventro-dorsal projection, showing the presence of an area with partially defined limits and greater radiopacity, measuring around 7.0cm in diameter, located between the 6th and 11th right intercostal space; (B) right latero-lateral projection, showing cardiac silhouette within normal radiographic standards, preserved lumen and tracheal pathway, slight amount of gaseous content in the esophageal pathway (C) left latero-lateral projection, showing degeneration of the costal cartilages and osteoarthritis of the costochondral joints, deforming ventral spondylosis at T6-7, heterogeneous content (suggestive of food content) in the gastric cavity.



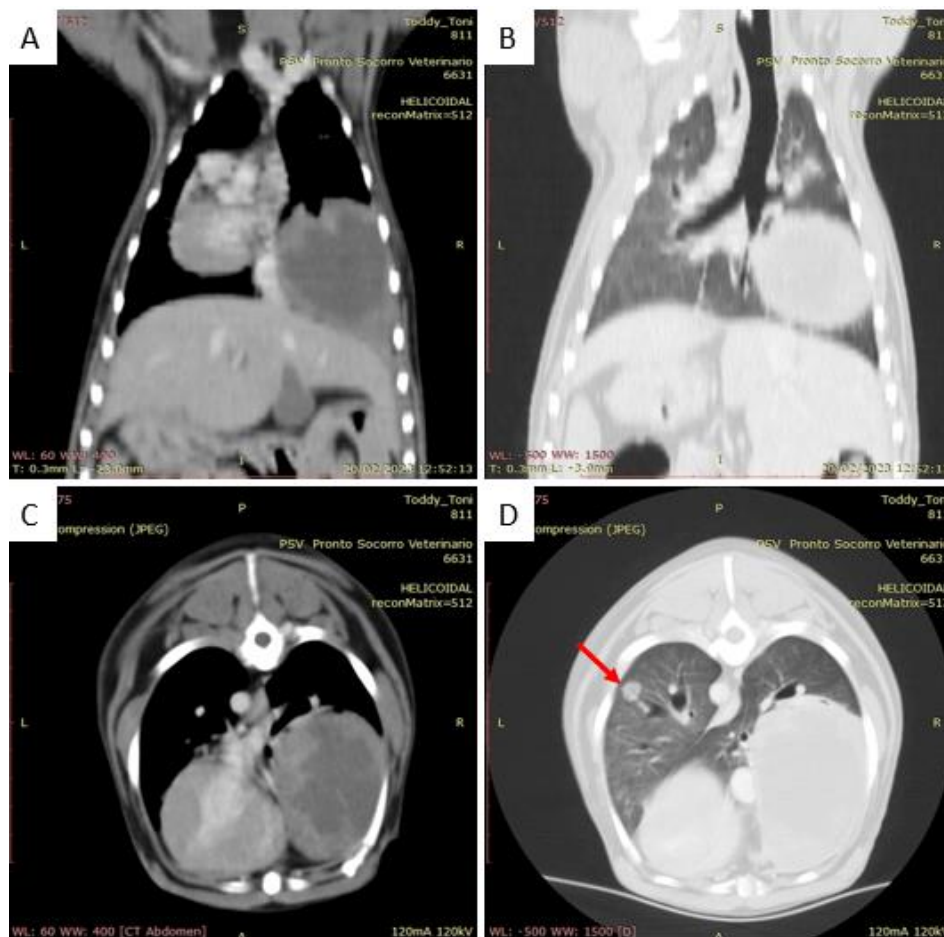
Fonte: (Silva Júnior et al., 2024).

The animal was treated with antibiotics (Amoxicillin + potassium clavulanate 20mg/Kg/B.I.D.; Metronidazole 15mg/Kg/B.I.D.), steroidal antiphlogistic (Prednisolone 1mg/Kg/S.I.D.), analgesic (Dipyrene 25mg/Kg/T.I.D.) for five days.

Based on the changes obtained on the x-ray, a computed tomography (CT) scan was performed on 2023/02/20 to better delineate the lesions and establish surgical planning. The CT showed: a soft tissue attenuation mass, with irregular margins and defined limits, showing enhancement with vascular contrast medium (Omnipaque 300mg/ml, at a dose of 1.5mg/kg), a bronchial component on the periphery and a cavitary

area interspersed, located in the ventral portion of the right caudal pulmonary lobe, extending from the fourth to the sixth costal arch, measuring 5cm in length x 6cm in height x 4cm in thickness. Furthermore, the mass made medial contact with the heart and caudal vena cava, causing slight compression on it; lateral and ventral contact with the chest wall; dorsal contact with the right main bronchus, causing slight compression on it; and caudal contact with the diaphragm, an area of linear atelectasis in the right cranial lobe and absence of lymph node enlargement. These findings led to a suggestive diagnosis of pulmonary neoplasia. In addition, a solid pulmonary nodule was visualized, with soft tissue attenuation, regular margins and defined limits, located in the dorsal portion of the peripheral and dorsal left caudal lobes, measuring 0.65cm in diameter (red arrow), suggestive of metastasis (figure 2).

Figure 2 - Computed tomography scan of a SRD dog. (A) Dorsal section with soft tissue window in contrasted series and visualization of soft tissue attenuation mass, defined limits, located in the ventral portion of the right caudal pulmonary lobe showing enhancement to the vascular contrast medium and cavitary area in the center, the formation makes medial contact with the heart and caudal vena cava; (B) dorsal section in contrasted series and visualization of mass in lateral and ventral contact with the chest wall, dorsal contact with the right main bronchus, caudal contact with the diaphragm. Extending from the fourth to the sixth costal arch, measuring 5cm long x 6cm high x 4cm thick. (C) Cross-section with lung window in contrasted series and visualization of soft tissue attenuation mass, defined limits, located in the ventral portion of the right caudal lung lobe; (D) Cross-section with lung window showing solitary soft tissue attenuation pulmonary nodule in the dorsal and peripheral portion of the left caudal lung lobe, suggestive of metastasis.

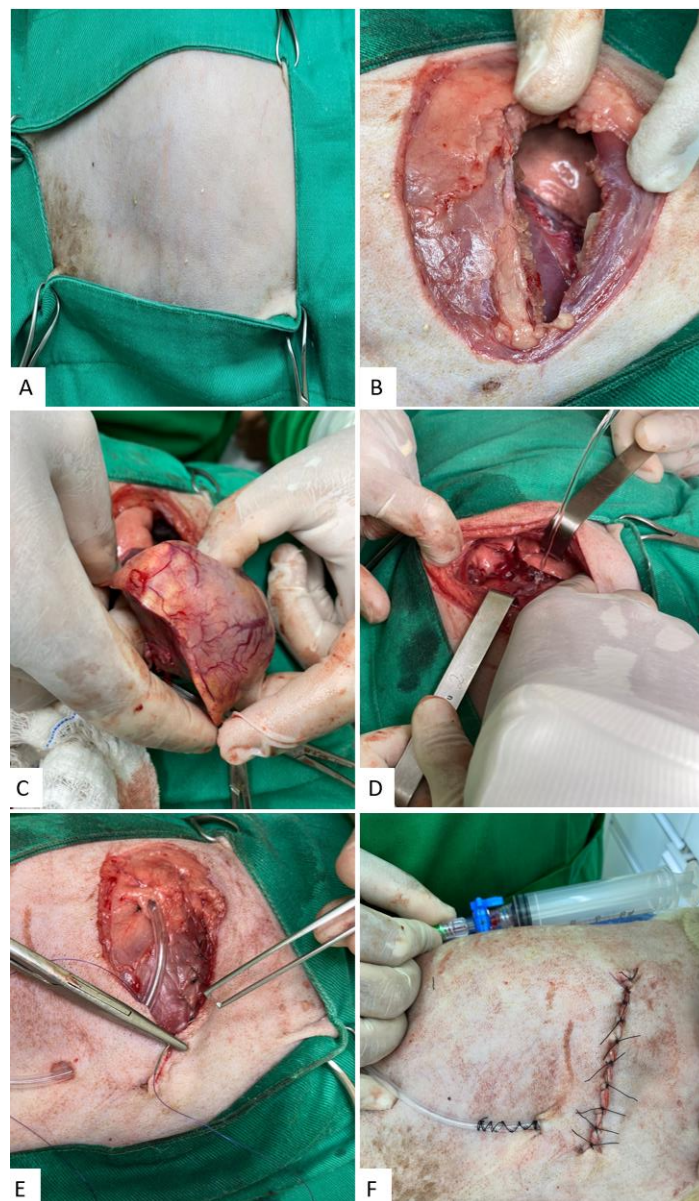


Fonte: (Silva Júnior et al., 2024).

The surgery for lobectomy of the right caudal lung lobe was carried out on 2023/03/06, with the patient already in venoclysis and properly prepared for the procedure, pre-anesthetic medication (PAM) was administered, combining Methadone 0.25mg/Kg with Midazolam 0.25mg/Kg intramuscularly (IM). Induction was followed by intravenous (I.V) administration of (Propofol) 5mg/Kg and maintenance with isoflurane associated with 100% oxygen at a sufficient dose to keep the animal in the proper surgical anesthetic plane, the 3rd plane of the 3rd stage of anesthesia as described by Guedel (1937). At the same time, a 0.9% NaCl solution was applied in a volume of 500mL with 2mL of 50µm/mL fentanyl citrate, 7.5mL of 2% lidocaine hydrochloride and 0.35mL of 10% ketamine hydrochloride (FLK), using an infusion rate of 10mL/kg/h, i.e. 0.03µg/kg/min of fentanyl, 50µg/kg/min of lidocaine and 10µg/kg/min of ketamine adjusted on an infusion pump, during the trans- and immediate post-operative periods.

With the surgical field duly prepared and the animal positioned in the left lateral decubitus position (figure 3a), an infiltrative local anesthetic block (Bupivacaine 0.2mg/Kg) was performed at the level of the 5th right intercostal space. An incision was made in this same area to access the thoracic cavity (figure 3b). With the aid of Farabeuf retractors, the ribs were pulled apart in order to locate the approximately 10cm-circumference nodule in the right caudal pulmonary lobe (figure 3c), which was then bluntly dissected in relation to the middle mediastinum and the caudal vena cava in order to promote hemostasis and aerostasis. For definitive hemostasis of the blood vessels, simple ligatures were made and for aerostasis, a mattress pattern suture was superimposed on a simple continuous suture, both using 3-0 polyglecaprone thread. After removing the lung lobe, the thoracic cavity was washed with 0.9% NaCl saline solution heated to 39°C (figure 3d), followed by the installation of a thoracic drain to restore negative pressure and drain fluids (figure 3e). The surgical incision was closed using a standard Sultan suture with 2-0 nylon thread in the intercostal muscles, a standard zig-zag suture with 2-0 polyglecaprone thread in the subcutaneous tissue and a separate simple standard suture with 2-0 nylon thread in the skin. The drain was fixed to the skin using a ballerina suture with 2-0 nylon thread (figure 3f).

Figure 3 - Exploratory thoracotomy for removal of a nodule present in the ventral portion of the right caudal pulmonary lobe of a SRD dog. (A) Surgical field showing trichotomy of the area and fixation of the cloth and field; (B) Thoracotomy to access the lobe affected by the nodule; (C) exteriorization of the nodule present in the ventral portion of the right caudal pulmonary lobe; (D) thoracic cavity washing process after confirming aerostasis; (E) positioning of the drain to drain the fluid, maintain negative pressure and abolish dead space; (F) thorax duly closed with a simple continuous suture pattern with 2-0 nylon.

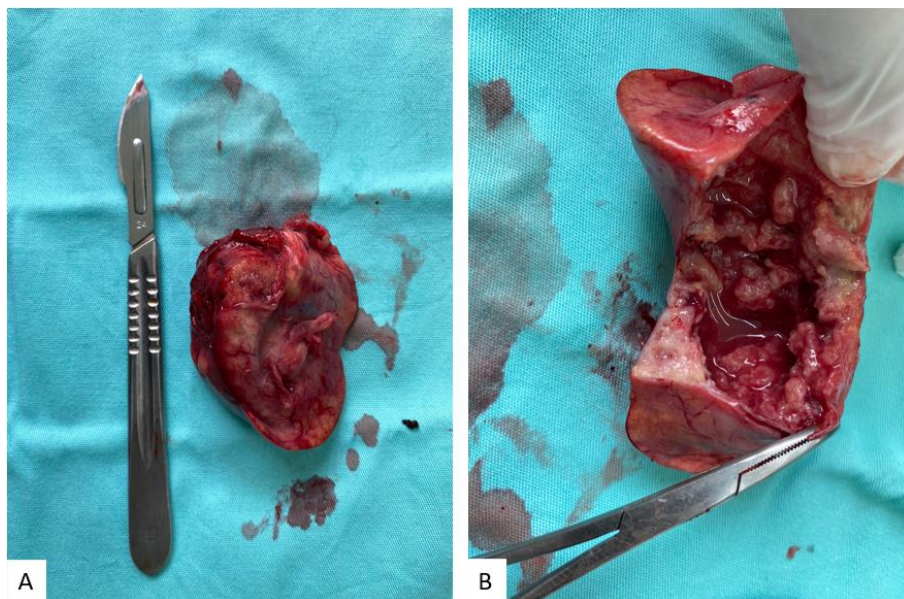


Fonte: (Silva Júnior et al., 2024).

In the immediate post-operative period, around 10mL of fluid was drained from the chest. Pain control in the immediate postoperative period was provided (Methadone 0/5mg/Kg/T.I.D.; Dipyrrone 25mg/Kg and Meloxicam 0.1mg/Kg/ both S.I.D) subcutaneously (S.C). The animal was kept in hospital for 120 hours, receiving antibiotic therapy (Ceftriaxone 30mg/Kg/B.I.D.; Metronidazole 15mg/Kg/B.I.D; Enrofloxacin 5mg/Kg/B.I.D) associated with antiphlogistic (Meloxicam 0.1mg/Kg/S.I.D) in addition to analgesics (Tramadol 4mg/Kg/B.I.D and Dipyrrone 25mg/Kg/T.I.D). Local dressings were also applied twice a day, cleansing with 0.9% NaCl saline solution, followed by the application of Vetaglós ointment® until the stitches were removed after 14 days. The chest tube was kept in place for 96 hours due to the cessation of chest fluid production.

After resection of the nodule (figure 4a), the sample was submitted to a general macroscopic assessment, fixed in 10% formaldehyde solution and sent for histopathological and immunohistochemical assessment. On sectioning the nodule, a bloody yellow liquid was released, suggestive of an abscess (figure 4b).

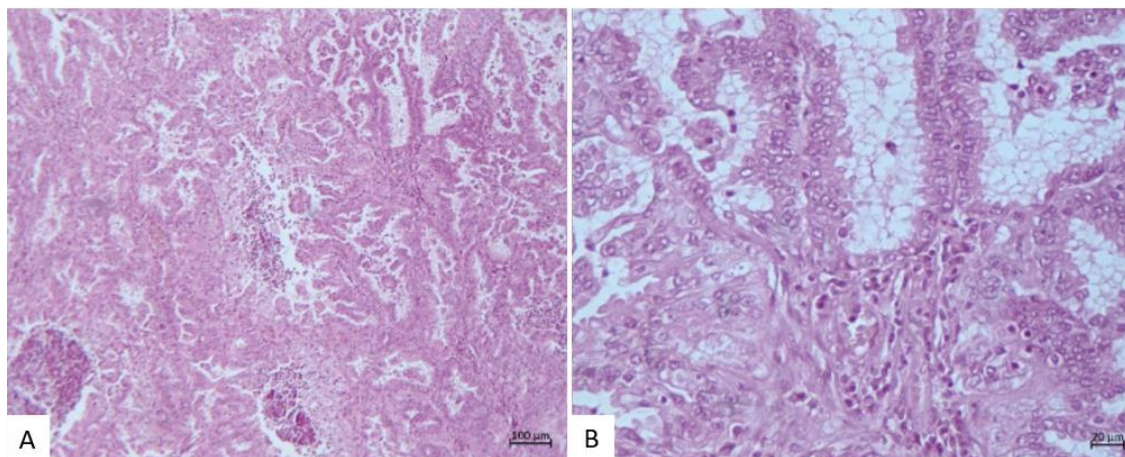
Figure 4 - General macroscopic inspection of a neoformation present in the ventral portion of the right caudal pulmonary lobe of a SRD dog. (A) Excisional biopsy of a pulmonary nodule approximately 7cm in diameter, adhered, smooth surface, soft consistency, non-hyperpigmented, showing a central cystic area; (B) Cross-section of a cystic nodule showing bloody yellow content.



Fonte: (Silva Júnior et al., 2024).

Histologically, alveolar parenchyma dissociated by neoplastic proliferation of pulmonary epithelial cells, with marked anisocytosis and anisokaryosis, non-circumscribed, organized into papillae and occasional acini, occasionally filled with cellular debris, marked neutrophilic inflammatory infiltrate or amorphous pink material. The cells have abundant cytoplasm, similar to stratified epithelium, containing small vacuoles that do not stain, round, hyperchromatic nuclei, open chromatin and obvious nucleoli of varying sizes. Binucleated cells and karyomegaly present. Atypical mitosis figures, slight fibroplasia, multifocal areas of necrosis. Emboli of neoplastic cells were identified in blood vessels (figure 5a,b).

Figure 5 - Photomicrographs of nodule in the ventral portion of the right caudal lung lobe, SRD dog. (A) Lung parenchyma invaded by neoplastic proliferation of pulmonary epithelial cells in papillary formation; (B) Neoplastic epithelial cells with marked anisocytosis and anisokaryosis, binucleated cells and karyomegaly. Figure of atypical mitosis and neutrophilic inflammatory infiltrate. Hematoxylin-eosin (HE) stain. Scale 100x and 400x.

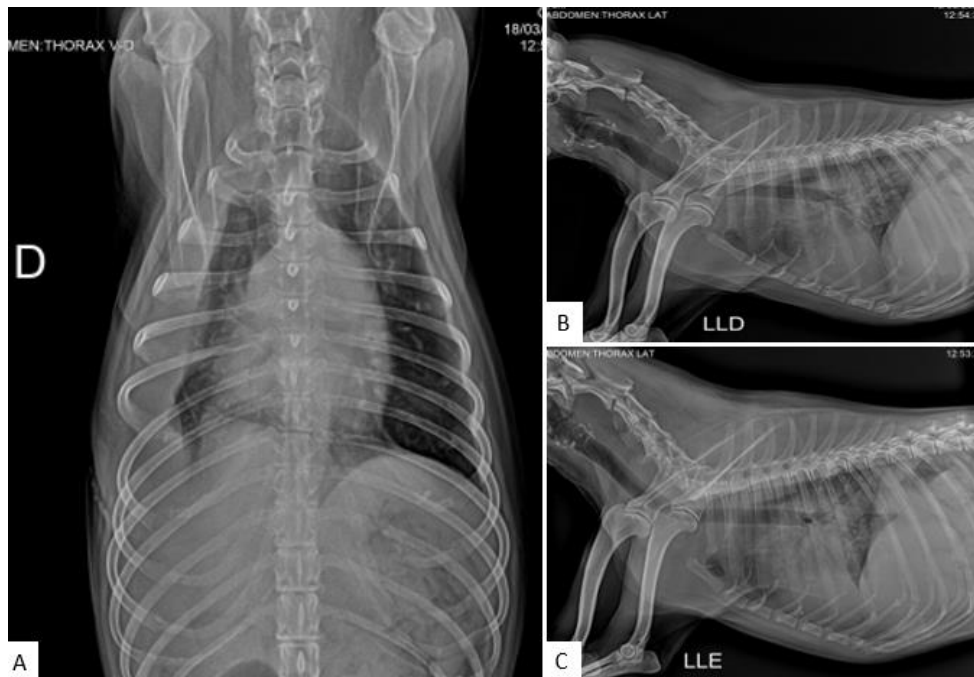


Fonte: (Silva Júnior et al., 2024).

On 2023/03/18, twelve days after the surgery, the animal was clinically re-evaluated and presented with nasal discharge, a productive cough, sporadic vomiting, anorexia and prostration. On general clinical examination, the animal was ECC (5.0), normocardic (100bpm), normopneic (40mrpm), hyperthermic (39.5°C), moderately dehydrated (8 - 9%), anorexic, with hypochromic mucous membranes, hypodipsia, oliguria and normoquesia. On this date, another x-ray was carried out, showing a liquid collection in the right hemithorax , diffuse opacification of the right lung fields that could be assessed as an interstitial pattern

(this could be related to atelectasis secondary to pleural effusion), cardiac silhouette within normal radiographic standards, preserved lumen and tracheal path, degeneration of the costal cartilages and osteoarthritis of the costochondral joints (suggestive of senescence), deforming ventral spondylosis at T6-7 and preservation of the bony structures of the rib cage (figure 6).

Figure 6 - Second chest X-ray in three projections of a SRD dog. (A) ventro-dorsal projection showing a liquid collection in the right hemithorax; (B) right latero-lateral projection, showing diffuse opacification of the right lung fields that could be assessed for interstitial pattern and cardiac silhouette within normal radiographic standards, preserved lumen and tracheal path (C) left latero-lateral projection, degeneration of the costal cartilages and osteoarthritis of the costochondral joints, deforming ventral spondylosis at T6-7 and preservation of the bony structures of the rib cage.



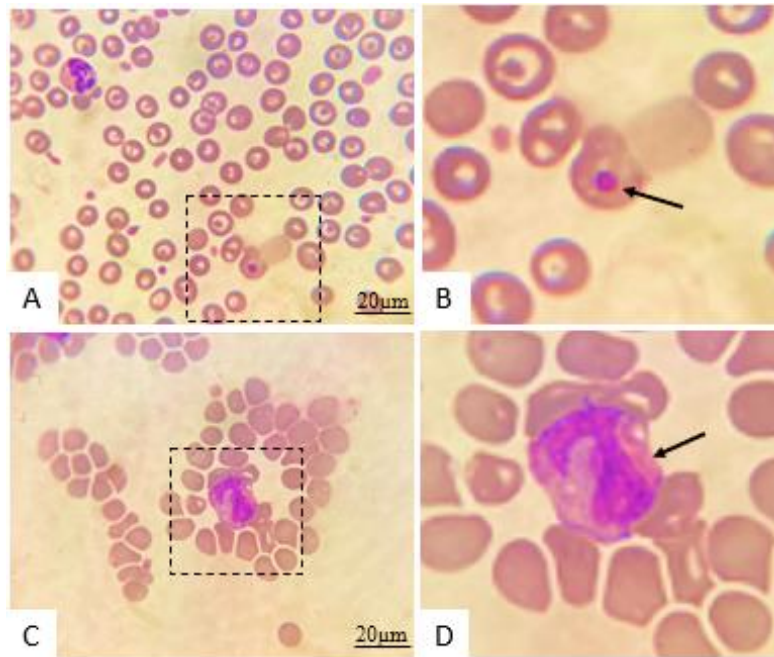
Fonte: (Silva Júnior et al., 2024).

After confirming the presence of fluid in the right hemithorax, it was drained by thoracentesis, between the 4th and 6th intercostal spaces, in the amount of 40mL, with a serosanguineous characteristic.

In addition, new hematological tests (blood count and biochemistry) were performed. The blood count showed regenerative anemia (erythrocytes 2.87mm^3 macrocytic and normochromic, hemoglobin 7.5mm^3 and globular volume 23.5mm^3), a leukogram with leukopenia (4100mm^3) and biochemical tests (creatinine, urea, ALT and

FA) and platelets without alterations. Also, microscopic evaluation for differential leukocyte count showed viral inclusions in erythrocytes (figure 7) and neutrophils (figure 7b) compatible with Lentz corpuscle, characterizing infection by the distemper virus. The animal was re-admitted to hospital after 48 hours for correction of dehydration and esophageal probing to administer food. Antibiotic therapy was prescribed (Ceftriaxone 30mg/Kg/B.I.D.; Enrofloxacin 5mg/Kg/B.I.D) antiphlogistic (Meloxicam 0.1mg/Kg/S.I.D) plus analgesics (Tramadol 4mg/Kg/B.I.D and Dipyrone 25mg/Kg/T.I.D). At the end, the animal died on 2023/03/22, possibly as a result of complications from the metastasis of the adenocarcinoma and enhanced by the lung lesions caused by the canine distemper virus, diagnosed during the post-operative treatment of the lung neoplasm. The owner did not authorize a necropsy to be carried out on the animal, but did sign an informed consent form agreeing to provide the images and relevant information for this case report.

Figure 7. Blood sample for differential leukocyte count, showing intracytoplasmic inclusions of Corpuscle of Lentz in the blood of a SRD dog. (A) Intra-erythrocytic inclusion of Corpuscle of Lentz; (B) Selection of the area of the dotted box with emphasis on the intra-erythrocytic structure marked by the black arrow; (C) Intra-leukocytic inclusion of Corpuscle of Lentz; (D) Selection of the area of the dotted box with emphasis on the intra-erythrocytic structure-stained pink, pointed by the black arrow. Quick panoptic stain. Scale 100x.



Fonte: (Silva Júnior et al., 2024).

DISCUSSION

We consider that the clinical manifestations presented by the animal were non-specific, and the clinical findings alone were not enough to determine any diagnosis. In this sense, we noticed that the clinical alterations were only considered by the owners when the neof ormation had already reached a considerable size of approximately 7cm in the affected lobe. According to Leandro et al. (2015) and Lorch et al. (2019), primary lung neoplasms have a silent clinical course and represent an important challenge to the clinician, often with a guarded to unfavorable prognosis, when these neoplasms are found at a very advanced stage of development, concomitantly, when the first signs and symptoms are recognized, the most reported being dyspnea (6% to 24%) and cough (52% to 93%). Conti et al. (2010) point out that around 25% of dogs with primary pulmonary neoplasms are often diagnosed as an

incidental finding during thoracic radiographic evaluation for non-specific alterations, or during routine examinations, especially in senile animals.

Animals over the age of 10 represent the largest number of animals suffering from lung neoplasms (da Silva et al., 2012; Leandro et al., 2015; Pereira et al., 2020), corroborating to the findings of this study. Santos et al. (2013) in their studies show that the increased prevalence of neoplasms was correlated with the greater longevity of dogs, and that breed could also predispose to the development of specific types of tumors, especially in Boxer breed dogs. Different findings were also found by Da Silva et al. (2012) when lung adenocarcinomas were reported in an eight-year-old dog of no defined breed. The literature mentions that racial and sexual factors are not predictors of the prevalence of cases in dogs (MANIAM et al., 2018; PEREIRA et al., 2019), however, studies indicate that the Boxer, Labrador, Springer Spaniel, Golden Retriever and Setter breeds seem to be more affected (Sato et al., 2005), and have also been cited in dogs of the Dobermann, Australian Shepherd and Bernese Cattle breeds (da Silva et al., 2012). We believe that this correlation may be associated with the faster onset of senility in these medium to large breeds, compared to small or miniature dogs.

The neutrophilic leukocytosis diagnosed in the animal in this report, in its first clinical and laboratory evaluation, may be correlated with the intratumoral inflammatory process (abscess) of the neoplastic development itself. Tamura et al. (2022), evaluating leukocytosis in dogs affected by lung adenocarcinoma and paraneoplastic syndromes, showed that in these patients, there is a significant increase in the expression of granulocyte colony-stimulating factor (G-CSF) and interleukin (IL6), and added that this increase may be related to a guarded to unfavorable prognosis in the affected animals. These findings are reported in lung adenocarcinomas in humans, because they are rapidly proliferating and refractory to chemotherapy treatment, resulting in an unfavorable prognosis (KASUGA et al., 2001; KAWAKAMI et al., 2020). According to Chaudhuri, (1973) primary lung neoplasms can produce abscesses or cysts in two ways: cavitory necrosis, due to the breakdown of the tumor growth itself; stenotic abscess, due to infection and rupture of the lung parenchyma distal to the bronchial obstruction, also caused by tumor growth, in both of which, findings of neutrophilic leukocytosis are common.

One of the possibilities for diagnosing lung adenocarcinomas in dogs, even before surgical treatment, which is the standard treatment, is ultrasound-guided cytology. Taking the imaging findings obtained in this report as a parameter, based on X-rays and CT scans showing a solitary nodule in the right caudal lung lobe, it was possible to determine its size and invasiveness, facilitating surgical excision with a safe surgical margin. Although it's

possible to diagnostic using cytology, some disadvantages have already been reported. According to Conti et al. (2010), collecting material through guided cytology can lead to serious complications, such as hemothorax or pneumothorax. Leandro et al. (2015), on the other hand, despite having used guided cytology as a diagnostic tool, the cytological analysis of the material did not guarantee a conclusive diagnosis, revealing inflammatory and degenerated cells, even though interferences with the procedure were not reported. The rates at which cytology aspirates guided by ultrasound or CT provide a diagnosis range from 38% to 90% of cases, and this variation is related to the accessibility of the tumor and the quality of the aspirate (LOCH et al., 2019).

There were no complications in the trans-operative period, nor in the immediate post-operative period. The anesthetic protocol and surgical technique used to partially remove the affected lobe were effective in this report, with no other complications such as hemorrhage, pneumothorax, pyothorax, infections or subcutaneous emphysema. Different anesthetic protocols have been used for the surgical treatment of lung adenocarcinoma in dogs, with different survival rates (LEANDRO et al., 2015; PEREIRA et al., 2020).

The definitive diagnosis of Papillary Lung Adenocarcinoma in this report was established by histopathological evaluation. According to Tisi et al. (1983), the histopathological examination makes it possible to determine the histological type and tissue invasion, indicate staging, appropriate treatment and predict the prognosis of each case. According to Capelozzi (2009), immunohistochemistry is an important complementary tool in the routine diagnosis of lung tumors and for identifying the different undifferentiated histological types, as well as determining prognostic factors, selecting individuals for appropriate oncological treatment and indicating the risk of recurrence and disease progression.

The average survival rate in dogs with lung tumors is 345 days for localized disease without infiltration into adjacent tissues, and even remission of the disease can be achieved by surgical intervention. In contradiction, survival is only 60 days when sentinel lymph nodes are involved (Lorch et al., 2019). Different animal survival rates are reported in surgically treated dogs associated or not with concomitant chemotherapy or infections. Leandro et al. (2015) reported a 90-day survival rate in a dog without chemotherapy treatment. Pereira et al. (2019) reported a 10-month survival rate in a dog diagnosed with lung neoplasia undergoing chemotherapy with alternating Gemcitabine and Carboplatin.

The survival of the dog in this report was only 16 days. We believe that the infection by the distemper virus occurred during the course of the animal's recovery, facilitated by the delay in the vaccination protocol for polyvalent immunization. This infection, in addition to

the presence of tumor emboli in pulmonary blood vessels, impaired the maintenance of lung function or integrity, hampering the animal's recovery. According to De Vries et al. (2015), the canine distemper virus has a high infectious activity due to its affinity for neural, lymphocytic and epithelial cells, and can affect not only the nervous system, but also the respiratory and gastroenteric systems, capable of causing profound immunosuppression. To date, there have been no reports of an association between dogs diagnosed with lung tumors and those co-infected with canine distemper virus.

CONCLUSION

Lobular excision used in the treatment and control of Papillary Lung Adenocarcinoma is effective, but infection by the distemper virus during the course of recovery from surgical treatment impairs the animal's recovery and survival.

REFERENCES

ABLE, H. et al. Computed tomography radiomic features hold prognostic utility for canine lung tumors: An analytical study. **PloS one**, v. 16, n. 8, p. e0256139, 2021. <https://doi.org/10.1371/journal.pone.0256139>

CAPELOZZI, V. L. Papel da imuno-histoquímica no diagnóstico do câncer de pulmão. **Jornal Brasileiro de Pneumologia**, v. 35, p. 375-382, 2009. <https://doi.org/10.1590/S1806-37132009000400012>

CHAUDHURI, M. Ray. Primary pulmonary cavitating carcinomas. **Thorax**, v. 28, n. 3, p. 354-366, 1973. <https://doi.org/10.1136/thx.28.3.354>

CONTI, M. B. et al. A case of primary papillary disseminated adenocarcinoma of canine lung. **Veterinary research communications**, v. 34, p. 111-115, 2010. <https://doi.org/10.1007/s11259-010-9378-1>

DALECK, C. R.; De NARDI, A. B. **Oncologia em cães e gatos**. 2a ed. Rio de Janeiro: Roca, 2016. 766p.

DA SILVA, E. O. et al. Tumor primário pulmonar metastático em três cães. **Semina: Ciências Agrárias**, v. 33, n. 2, p. 3271-3278, 2012. <https://doi.org/10.5433/1679-0359.2012v33Supl2p3271>

DEVARAKONDA, S. et al. Genomic profiling of lung adenocarcinoma in never-smokers. **Journal of Clinical Oncology**, v. 39, n. 33, p. 3747-3758, 2021. <https://doi.org/10.1200/jco.21.01691>

DE VRIES, Rory D.; DUPREX, W. Paul; DE SWART, Rik L. Morbillivirus infections: an introduction. **Viruses**, v. 7, n. 2, p. 699-706, 2015. <https://doi.org/10.3390/v7020699>

GUEDEL, Aruthur E. Inhalation Anesthesia: A Fundamental Guide. **Anesthesia & Analgesia**, v. 16, n. 2, p. 119-120, 1937.

IGUCHI, A. et al. Suspected eccrine adenocarcinoma on footpad of the right hindlimb in a dog. **Journal of Veterinary Medical Science**, v. 81, n. 6, p. 821-823, 2019. <https://doi.org/10.1292/jvms.18-0286>

KANAI, E. et al. Video-assisted thoracic surgery anatomical lobectomy for a primary lung tumor in a dog. **Journal of Veterinary Medical Science**, v. 81, n. 11, p. 1624-1627, 2019. <https://doi.org/10.1292/jvms.19-0412>

KASUGA, I. et al. Tumor-related leukocytosis is linked with poor prognosis in patients with lung carcinoma. **Cancer**, v. 92, n. 9, p. 2399-2405, 2001. [https://doi.org/10.1002/1097-0142\(20011101\)92:9%3C2399::AID-CNCR1588%3E3.0.CO;2-W](https://doi.org/10.1002/1097-0142(20011101)92:9%3C2399::AID-CNCR1588%3E3.0.CO;2-W)

KAWAKAMI, N. et al. IL-6 and G-CSF production resulting from lung cancer in an HIV patient. **IDCases**, v. 19, p. e00693, 2020. <https://doi.org/10.1016/j.idcr.2020.e00693>

KISHI, E. N. et al. Functional metastatic parathyroid adenocarcinoma in a dog. **The Canadian Veterinary Journal**, v. 55, n. 4, p. 383, 2014. <http://www.ncbi.nlm.nih.gov/pmc/articles/pmc3953943/>

KITA, C. et al. Immunohistochemical features of canine ovarian papillary adenocarcinoma and utility of cell block technique for detecting neoplastic cells in body cavity effusions. **Journal of Veterinary Medical Science**, v. 84, n. 3, p. 406-413, 2022. <https://doi.org/10.1292/jvms.21-0633>

LEANDRO, R. M. et al. Carcinoma pulmonar adenoescamoso em cão - Relato de Caso. **Uniciências**, v. 19, n. 2, 2015. <https://doi.org/10.17921/1415-5141.2015v19n2p%25p>

LEE, B. M. et al. Retrospective evaluation of a modified human lung cancer stage classification in dogs with surgically excised primary pulmonary carcinomas. **Veterinary and Comparative Oncology**, v. 18, n. 4, p. 590-598, 2020. <https://doi.org/10.1111/vco.12582>

LEE, H. et al. A case of gastric adenocarcinoma in a Shih Tzu dog: successful treatment of early gastric cancer. **Journal of Veterinary Medical Science**, v. 76, n. 7, p. 1033-1038, 2014. <https://doi.org/10.1292/jvms.13-0315>

LORCH, G. et al. Identification of recurrent activating HER2 mutations in primary canine pulmonary adenocarcinoma. **Clinical Cancer Research**, v. 25, n. 19, p. 5866-5877, 2019. <https://doi.org/10.1158/1078-0432.ccr-19-1145>

MANIAM, R. et al. Pulmonary papillary adenocarcinoma with *Aspergillus versicolor* infection in a dog. **Medical mycology case reports**, v. 19, p. 25-29, 2018. <https://doi.org/10.1016/j.mmcr.2017.11.005>

MEUTEN, D. J. (Ed.). **Tumors in domestic animals**. John Wiley & Sons, 2020.

PALLADINO, S. et al. Utility of computed tomography versus abdominal ultrasound examination to identify iliosacral lymphadenomegaly in dogs with apocrine gland adenocarcinoma of the anal sac. **Journal of Veterinary Internal Medicine**, v. 30, n. 6, p. 1858-1863, 2016. <https://doi.org/10.1111/jvim.14601>

PEDROSO, T. C. et al. Adenocarcinoma papilar de pulmão em cão: Relato de caso. **Pubvet**, v. 4, p. Art. 938-943, 2010.

PEREIRA, L. B. de S. B. et al. Aspectos clínicos, diagnóstico e tratamento do adenocarcinoma pulmonar canino: relato de caso. **Medicina Veterinária (UFRPE)**, v. 13, n. 4, p. 514-520, 2019. <https://doi.org/10.26605/medvet-v13n4-3659>

ROCHA, J. et al. Carcinoma broncoalveolar com metástase intracraniana em cão: Relato de caso. **Enciclopédia Biosfera**, v. 9, n. 17, 2013.

SALVADO, I. S. de S. **Estudos retrospectivos das neoplasias em canídeos e felídeos domésticos, analisadas pelo laboratório de anatomia patológica da faculdade de medicina veterinária da Universidade Técnica de Lisboa no período compreendido entre 2000 e 2009**. 2010. 109f. Dissertação (Mestrado integrado em Medicina Veterinária). Universidade de Lisboa, Lisboa, 2010.

SANTOS, I. F. C. et al. Prevalência de neoplasias diagnosticadas em cães no Hospital Veterinário da Universidade Eduardo Mondlane, Moçambique. **Arquivo Brasileiro de Medicina Veterinária e Zootecnia**, v. 65, p. 773-782, 2013. <https://doi.org/10.1590/S0102-09352013000300025>

SATO, T. et al. Pulmonary adenosquamous carcinoma in a dog. **Journal of Veterinary Medicine Series A**, v. 52, n. 10, p. 510-513, 2005. <https://doi.org/10.1111/j.1439-0442.2005.00773.x>

TAMURA, K. et al. Neutrophilic leucocytosis induced by granulocyte colony-stimulating factor and interleukin-6 in canine primary lung adenocarcinoma. **Veterinary Medicine and Science**, v. 8, n. 2, p. 483-491, 2022. <https://doi.org/10.1002/vms3.694>

TISI, G. M. et al. Clinical staging of primary lung cancer. **American Review of Respiratory Disease**, v. 127, n. 5, p. 659-664, 1983. <https://doi.org/10.1164/arrd.1983.127.5.659>

VALENTI, P. et al. Evaluation of electrochemotherapy in the management of apocrine gland anal sac adenocarcinomas in dogs: A retrospective study. **Open Veterinary Journal**, v. 11, n. 1, p. 100-106, 2021. <https://doi.org/10.4314/ovj.v11i1.15>

VIGNOLI, M. et al. A case of adenocarcinoma of uterus masculinus in a Pomeranian dog. **Frontiers in Veterinary Science**, v. 7, p. 337, 2020.
<https://doi.org/10.3389/fvets.2020.00337>

WILSON, R.; DEVARAJ, A. Radiomics of pulmonary nodules and lung cancer. **Pulmonary Nodules and Lung Cancer**, p. 128, 2017.